Vietnam Journal of Earth Sciences, 48(1), 1–24, https://doi.org/10.15625/2615-9783/23795

Vietnam Journal of Earth Sciences
https://vjs.ac.vn/index.php/jse

Land use, land cover change intensity, and landscape fragmentation in the Western Nghe An Biosphere Reserve from 1990 to 2020

Tran Van Truong[1*], Dang Thi Ngoc[1], Nguyen Huu Duy[1], Pham Van Manh[1], Ngo Van Liem[1], Pham Viet Thanh[1], Nguyen Anh Duc[1], Nguyen Van Hong[2]

[1]*Faculty of Geography, University of Science, Vietnam National University, Hanoi, Vietnam*
[2]*Institute of Earth Sciences, VAST, Hanoi, Vietnam*

Received 01 November 2023; Received in revised form 06 August 2024; Accepted 14 November 2025

ABSTRACT

Land-use and land-cover (LULC) change, as well as landscape fragmentation, significantly impact biodiversity conservation in biosphere reserves. This paper aims to analyze LULC change intensity and landscape fragmentation, and to test their relationship within the Western Nghe An Biosphere Reserve (WNABR) from 1990 to 2020. LULC data from 1990, 2000, 2010, and 2020, covering 13 LULC types, were analyzed for LULC change, LULC change intensity at the interval and categorical levels, and landscape fragmentation using landscape metrics at class and landscape levels. Pearson's correlation coefficient was then employed to examine the relationship between land change intensity and landscape fragmentation. The results indicate that from 1990 to 2020, high-developed areas, low-developed areas, and bamboo areas consistently increased, while plantation land, scrub/shrub, grassland/herbaceous vegetation, other croplands, and rice paddies declined. Evergreen broadleaf forest areas remained stable and dominant. Land change intensity was above average from 1990 to 2000, then gradually decreased from 2000 to 2020. Evergreen broadleaf forests, open water, other croplands, and rice paddies exhibited lower land change intensity than other types. There is a general trend of decreasing fragmentation within the WNABR. Evergreen broadleaf forest and plantation land are composed of large, less fragmented patches, while the remaining LULC types are typically fragmented into small, scattered patches. LULC change intensity and landscape fragmentation increased from the core zone to the buffer and transition zones. There is a significant positive linear relationship between LULC change intensity and the number of patches (NP).

Keywords: Land use land cover, land change intensity, landscape fragmentation, Western Nghe An, biosphere reserve.

1. Introduction

The concept of biosphere reserves emerged in the early 1970s as a response to the growing threats to natural environments and the need to balance human activities with nature conservation (Van Cuong et al., 2017). These are areas that UNESCO has recognized for their outstanding natural and cultural values, and their potential to demonstrate innovative approaches to conservation and sustainable development (Batisse, 1997). Biosphere reserves are intended to serve as models of sustainable development,

*Corresponding author, Email: tranvantruong@hus.edu.vn

maintaining ecological integrity while supporting the social, economic, and cultural needs of local communities (Reed, 2019). As of 2020, there are 748 biosphere reserves in 134 countries, covering about 5% of the Earth's land surface (UNESCO, 2023b).

The biosphere reserve is organized into three interconnected zones: the core area, the buffer zone, and the transition area (Kušová et al., 2008). According to definitions, core zones are areas strictly reserved and protected by surrounding buffer zones, where traditional (low-impact) land-use practices are allowed, and transition zones, where more intensive land-use practices are gradually permitted (Batisse, 1982). Dynamic approaches to land use land cover (LULC) change are continuously assessed and monitored (Amini Parsa et al., 2016). Many studies have been conducted in biosphere reserves worldwide using satellite image data to determine LULC change, prediction of LULC change (Amini Parsa et al., 2016; Michel et al., 2021), landscape change and habitat quality (Clerici et al., 2007), the socioeconomic context of LULC change (Figueroa et al., 2009), management of LULC change (Walker & Solecki, 1999), monitoring landscape fragmentation and aboveground biomass estimation (Do et al., 2022). However, to date, no studies have analyzed LULC change intensity within biosphere reserves, nor have any elucidated the relationship between LULC change intensity and landscape fragmentation in these areas.

Analyzing land use and land cover (LULC) dynamics is key to understanding the interplay between human activities and the environment. The traditional transition matrix method analyzes changes in extent, size, and patterns of LULC, emphasizing significant transitions between land categories (Ettehadi Osgouei et al., 2022; Hu et al., 2019). However, this approach might overlook smaller, yet meaningful, changes. A more nuanced method is intensity analysis, as proposed by Aldwaik and Pontius Jr. (2012). This technique leverages transition matrices from different periods to provide a hierarchical analysis at the interval, category, and transition levels. Interval-level measures the speed of LULC changes within specific time intervals. The category level evaluates gains and losses across various land categories. The transition level offers detailed insights into transitions between land categories, highlighting targeted or avoided changes. This approach allows for a comprehensive understanding of land change dynamics, ensuring that both major and minor transitions are captured and understood (Aldwaik & Pontius, 2012). However, compared with research on LULC change using the transition matrix method, studies utilizing the intensity analysis method remain relatively rare.

Changes in land use and land cover (LULC) are arguably the most significant issue in many parts of the world. Dramatic LULC change is known to have a considerable impact on biodiversity, socioeconomic practices, water balance, ecosystem services, and regional climate (Duan et al., 2023; Rivas-Tabares et al., 2022; Sun et al., 2023). Changes in LULC led to habitat loss and fragmentation, which decreased biodiversity (Xu et al., 2018). Landscapes are composed of mosaics of natural and anthropogenic patches, whose spatial arrangement is referred to as landscape pattern (McGarigal, 2013). The dynamics of these patterns are typically described as landscape fragmentation-a process in which a contiguous patch of landscape is divided into smaller, isolated patches (Fischer & Lindenmayer, 2007). Landscape metrics are employed to quantify landscape patterns and fragmentation at patch, class, and landscape levels (Hargis et al., 1998; McGarigal, 2015). Given that no single spatial metric can fully capture landscape complexity, a selected set of metrics is often used to interpret landscape

patterns (Uuemaa et al., 2009). Landscape metrics provide a quantitative approach to measure fragmentation by evaluating various spatial characteristics of land cover patches (Frazier & Kedron, 2017). This process is crucial for understanding ecological impacts, planning sustainable land use, and implementing conservation strategies (McAlpine & Eyre, 2002; Uuemaa et al., 2009). While intensity analysis reflects changes in landscape pattern over time, it theoretically correlates with landscape fragmentation, as reflected in landscape metrics. Despite this, few studies have explored the relationship between LULC intensity and landscape metrics/landscape fragmentation.

Vietnam boasts 11 UNESCO-recognized biosphere reserves, spanning a total area of 4,900,661 hectares (UNESCO, 2023a). Among these, the Western Nghe An Biosphere Reserve (WNABR), covering 1,303,285 hectares (UNESCO, 2018), stands as the largest terrestrial biosphere reserve in the country, accounting for 26.6 percent of the total biosphere reserve area. Situated in a remote, mountainous region of central Vietnam, the WNABR is home to some of the nation's richest and most diverse flora and fauna. Due to its vast area and diverse population, the land use land cover (LULC) and landscape of WNABR are subject to changes driven by both natural and anthropogenic factors. However, no studies have yet assessed the effects of LULC changes on landscape fragmentation and biodiversity conservation in the WNABR.

This study aims to bridge this gap with the following specific objectives:

(i) Analyze the LULC intensity change from 1990 to 2020 for the entire WNABR and its functional zones.

(ii) Assess changes in landscape pattern and fragmentation from 1990 to 2020 for the entire WNABR and its functional zones.

(iii) Examine the relationship between LULC change intensity and landscape fragmentation, and its implications for biodiversity conservation in the WNABR.

2. Materials and methods

2.1. Description of study area

The Western Nghe An Biosphere Reserve, located in the remote western region of Nghe An Province within the Truong Son Mountain Range and bordering Laos (Fig. 1), spans approximately 1,303,285 hectares. It encompasses three core areas: a national park (Pu Mat) and two nature reserves (Pù Hoạt and Pu Huong). Additionally, it includes a buffer zone (503,270 hectares) and a transition zone (558,030 hectares) (Nguyen Tien Lam, 2016).

The entire WNABR falls within the administrative boundaries of nine mountainous districts of Nghe An Province, comprising 182 municipalities and 2,125 villages. According to the 2020 annual statistics, the biosphere reserve is home to around 2,000 people (Nghe An People Committee, 2021).

The topography of the WNABR is complex, divided by streams and rivers, and slopes gradually from the northwest to the southeast. Notable peaks in the region's western portion include Pu Hoat, Pu Mieng, Pu Samtie, Pu Tong Chinh, Pu Xong, and Pu Xai Lai Leng, with elevations ranging from 2,000 to 2,700 meters. Narrow plains and valley bottom surfaces, typically found at elevations of less than ten meters, are predominantly located along the Ca River and other nearby rivers and streams.

The area experiences a tropical humid monsoon climate, receiving 106 Kcal/cm² of total annual radiation, with an average yearly temperature of 23–24°C and 1,500–1,700 hours of sunshine. The region's average annual precipitation ranges from 1,200 to 2,000 mm, with 123–152 rainy days, and

yearly average humidity ranges from 80 to 90 percent.

The WNABR encompasses diverse habitats, including tropical rainforests, wetlands, and rivers. Closed mixed deciduous-coniferous forests are more prevalent at higher altitudes, while closed evergreen tropical rainforests are common below 700 meters. To date, 204 families and six phyla, comprising 2,615 plant species, have been identified in the area, including 59 rare species (Nghe An People Committee, 2017). Additionally, the region is home to 169 mammal species, 47 of which are rare, and 26 are classified as endangered by the IUCN (2000) (Hilton-Taylor & Brackett, 2000).

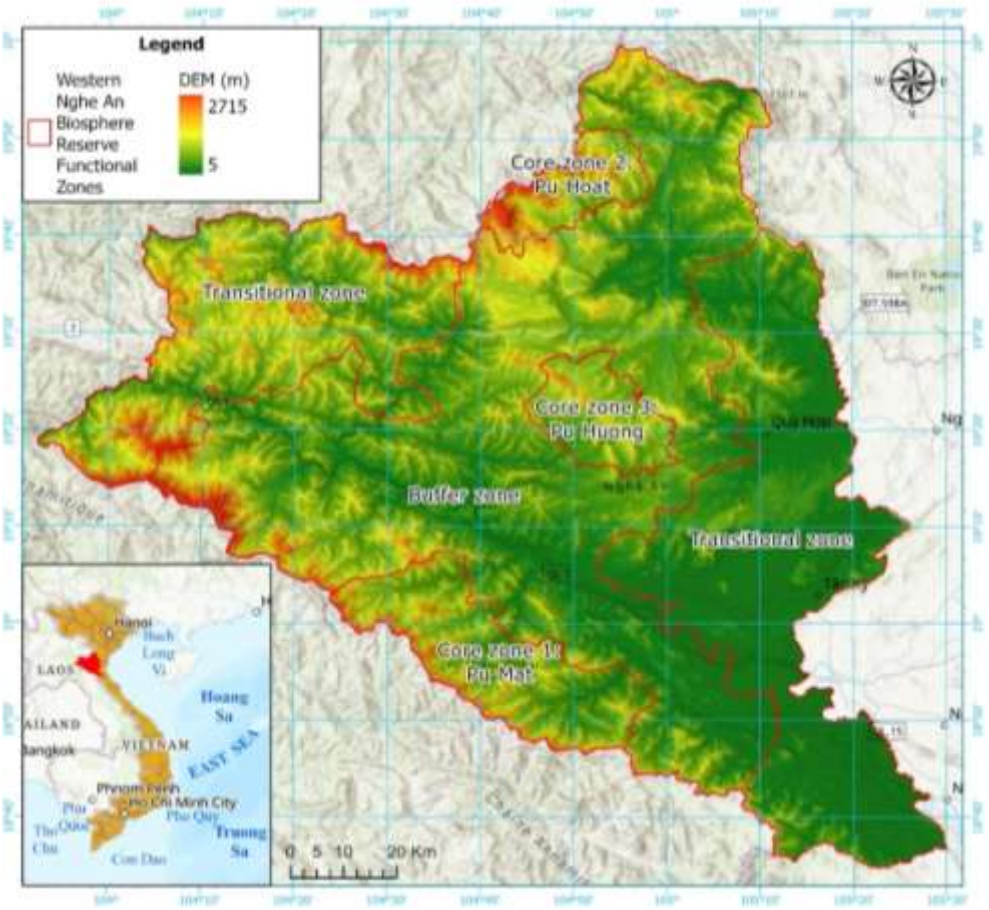

Figure 1. Location map of the Western Nghe An Biosphere Reserve

2.2. LULC data collection

The high-resolution land-use and land-cover dataset of Vietnam, version 21.09, published by the Japan Aerospace Exploration Agency (JAXA) Earth Observation Research Center (EORC), ALOS/ALOS-2 Science Project, and the "Earth Observation Priority Research: Ecosystem Research Group," was employed for this study. JAXA and EORC (ALOS/ALOS-2) began by developing 30-meter annual LULC raster datasets (VLUCDs) for the entire country of Vietnam using an innovative random forest-based algorithm with n_estimators = 200 (trees) and max_features = 8, among other default parameters, and various geospatial data sources, such as Sentinel-1 and Sentinel-2

imagery and Landsat data (JAXA et al., 2021).

The VLUCDs encompass a level-1 layer with ten distinct primary LULC classes and a level-2 layer with eighteen secondary LULC classes in Vietnam, comprising annual land cover products from 1990 to 2020. These datasets are independently verified using visual interpretation and field survey data. The overall accuracy of the level-1 layer ranges from 86 to 92 percent, while the The accuracy of Level-2 layers ranges from 78 to 85 percent (JAXA et al., 2021; Phan et al., 2021).

2.3. Methodology

Figure 2 presents the research framework, which includes four key processes.

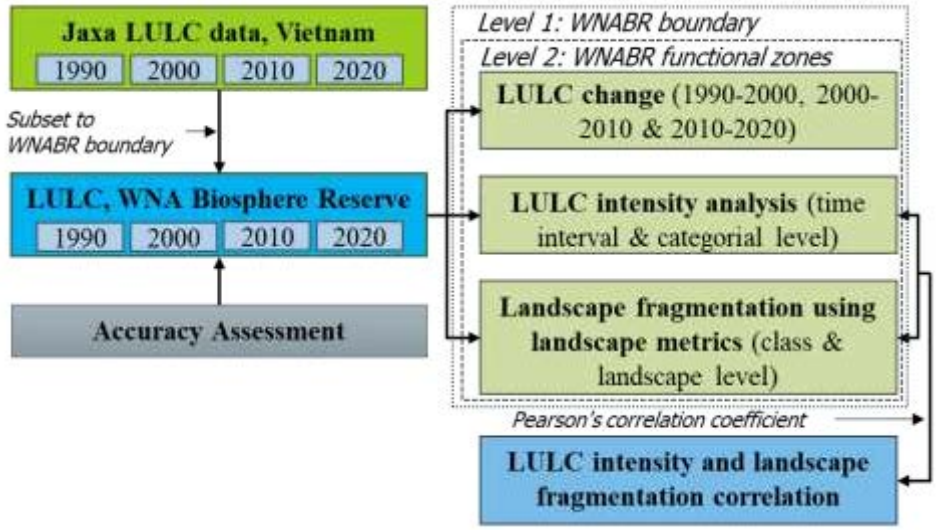

Figure 2. Flowchart of methodological framework

2.3.1. LULC change analysis

(i) LULC data processing

To evaluate the impact of LULC In biodiversity conservation, a diversity of habitats is preferred over a single forest type. Consequently, the 30-meter level-2 VLUCD raster datasets with 18 categories for all of Vietnam were freely downloaded from the JAXA EORC website (https://www.eorc.jaxa.jp/ALOS/en/dataset/lulc_e.htm#download). All LULC raster layers were projected to the Universal Transverse Mercator (UTM) map projection (Zone 48 N) and then clipped to the Western Nghe An Biosphere Reserve (WNABR) boundary to create a series of LULC maps at ten-year intervals (1990, 2000, 2010, and 2020). Four layers (1990, 2000, 2010, and 2020) with 13 LULC classes were obtained following this clipping process. Five classes were absent from the research area, compared with the 18 categories in the original LULC dataset across the entire country.

(ii) Accuracy assessment of LULC data

Despite the overall accuracy of the Given that 18-category VLUCD classification datasets for Vietnam range from 78 to 85 percent (JAXA et al., 2021; Phan et al., 2021), it remains crucial to assess the accuracy of the clipped LULC classification datasets for WNABR to evaluate the quality of information derived from the original data. To achieve this, the stratified random method was employed to represent the different LULC classes in the area.

The accuracy assessment used 750 reference points across 13 classes (30 points for small, separated classes; 50 points for large classes; and 100 points for extensive classes). Ground truth data were collected during field trips to the study area in 2021 and 2022. The research team traveled by car and motorcycle along main routes to survey points, taking photographs and noting information on habitats, main species, land use, and the economic activities of the local population. However, due to the extensive size of the study area and challenging terrain, ground-truth points were primarily collected along the edges of habitats. Therefore, it is crucial to extend the reference points using additional ancillary data, including high-resolution satellite images from Google Earth Pro, topographic maps, land-use maps, and forest maps of Nghe An Province published during the same period.

Validation points are randomly distributed throughout the study area based on the distribution of the classified 13 LULC types. This sampling strategy aligns with Congalton's (1991) recommendations. The LULC reference data and classification datasets were statistically compared using error matrices. The overall accuracy, users' and producers' accuracies, and the Kappa statistic were derived from these matrices. The Kappa index, which measures the extent of classification accuracy, was calculated using the formula provided by Rosenfield & Fitzpatrick-Lins (1986) (Eq. 1):

$$K = \frac{P(A)-P(E)}{1-P(E)} \quad (1)$$

where $P(A)$ is the relative observed agreement among raters, and $P(E)$ is the hypothetical probability of chance agreement (Foody, 2020).

(iii) LULC map and statistics

Following the accuracy assessment, all raster LULC layers were converted to vector format to determine the area (in hectares) and the contribution (in percent) of each LULC class within the study area. Furthermore, these LULC layers were overlaid on the WNABR functional zone layer to calculate the presence (in hectares) of LULC classes within core areas, buffer zones, and transition zones. This methodological approach ensures precise spatial analysis, enabling a comprehensive understanding of land-use dynamics across the biosphere reserve's functional zones.

(iv) LULC change detection

Following the production of LULC maps for WNABR for 1990, 2000, 2010, and 2020, the vector data from these maps were used to quantify LULC conversions across the following periods: 1990–2000, 2000–2010, 2010–2020, and 1990–2020.

A two-way cross-matrix, generated by executing the intersect procedure in ArcGIS 10.8, was used to identify the primary types of change within the study area. A new thematic layer was also created from the two 13-class LULC maps, encapsulating different combinations of "from-to" change classes. To monitor the most dynamic LULC, the percentage of net change was computed (Eq. 2):

$$p = \left(\frac{A_{t2}-A_{t1}}{A_{t1}*(t2-t1)}\right) *100 \quad (2)$$

where *p(%)* is the percentage of net change per year; A_{t1}, A_{t2} (hectares) are the area of the LULC type in the observation years, respectively ($t_1 < t_2$). Negative percentage values indicate a decline in area coverage, while positive values indicate an increase.

In addition, a zonal tabulation was performed to calculate changes in LULC classes across WNABR's functional zones from 1990 to 2020. Lastly, a Sankey multilevel diagram highlighted the significant LULC transfers between 1990 and 2020 (Fig. A.4).

2.3.2. LULC change intensity

The intensity analysis framework comprises interval, category, and transition

levels analyses. However, for this study, only interval- and category-level analyses were employed to examine LULC change intensity within the WNABR over 30 years (1990–2020).

(i) LULC change intensity analysis at the interval level

Intensity analysis uses land use change intensity *S(t)* (Eq. 3) and uniform intensity *U* (Eq. 4) to describe LULC changes over a specific period. If *S(t)* exceeds *U*, it indicates that land use change is occurring rapidly; conversely, if *S(t)* is less than *U*, land use change is slower (Aldwaik & Pontius, 2012; Anteneh et al., 2018).

$$S_t = \frac{Change\ during\ (Y_t,Y_{t+1})/area\ of\ study\ region}{(Duration\ of\ [Y_t,Y_{t+1}])(Extent\ size)} \times 100$$

$$= \frac{\left\{\sum_{J=1}^{J}\left[\left(\sum_{i=1}^{J} C_{tij}\right)-C_{tjj}\right]\right\}/\left[\sum_{J=1}^{j}\left(\sum_{i=1}^{J} C_{tij}\right)\right]}{Y_{t+1}-Y_t} \times 100 \quad (3)$$

$$U = \frac{area\ of\ change\ during\ all\ time\ intervals/area\ of\ study\ region}{Duration\ of\ all\ intervals} \times 100$$

$$= \frac{\sum_{t=1}^{T-1}\left\{\sum_{J=1}^{j}\left[\left(\sum_{i=1}^{J} C_{tij}\right)-C_{tjj}\right]\right\}/\left[\sum_{J=1}^{j}\left(\sum_{i=1}^{J} C_{tij}\right)\right]}{Y_T-Y_1} \times 100 \quad (4)$$

(ii) LULC change intensity analysis at the category level

Category-level analysis examines the intensity change of each land category within a specified time interval. It employs the annual gain intensity, Gtj (Eq. 5), and the annual loss intensity, Lti (Eq. 6), to elucidate land-use changes for a given land category (Aldwaik & Pontius, 2012; Anteneh et al., 2018). If *Gtj* or *Lti* exceeds U, the land category is considered active; otherwise, it is classified as dormant.

$$G_{ij} = \frac{area\ of\ gross\ gain\ of\ category\ j\ during\ [Y_i,Y_{t+1}]/Duration\ of\ [Y_t,Y_{t+1}]}{area\ of\ category\ j\ at\ time\ Y_{t+1}} \times 100$$

$$= \frac{\left[\left(\sum_{i=1}^{J} C_{tij}\right)-C_{tjj}\right]/[Y_t,Y_{t+1}]}{\left(\sum_{i=1}^{J} C_{tij}\right)} \times 100 \quad (5)$$

$$L_{ti} = \frac{area\ of\ gross\ gain\ of\ category\ I\ during\ [Y_i,Y_{t-1}]/Duration\ of\ [Y_t,Y_{t+1}]}{area\ of\ category\ j\ at\ time\ Y_{t+1}} \times 100$$

$$= \frac{\left[\left(\sum_{j=1}^{J} C_{tij}\right)-C_{tii}\right]/[Y_t,Y_{t+1}]}{\left(\sum_{j=1}^{J} C_{tij}\right)} \times 100 \quad (6)$$

In Eqs. 4-6, i and j denote the number of LULC categories, Ctij denotes the area that transformed from category i to category j at time t, and Yt denotes time.

2.3.3. Landscape pattern and fragmentation analysis

Four raster LULC layers in GeoTIFF format (1990, 2000, 2010, and 2020) of the WNABR were imported into the standalone software FRAGSTATS 4.0 to calculate landscape metrics. For each LULC raster layer, a set of 12 metrics from three categories (area-edge, shape, and aggregation) was estimated at the class level. In addition, 13 metrics in four categories (area-edge, shape, aggregation, and diversity) were measured at the landscape level (Table A.1). Two sampling strategies were set up to calculate the landscape metrics in Fragstats 4.0: a no-sampling strategy for the entire WNABR and an exhaustive sampling (user-provided tiles) for functional zones of the WNABR (McGarigal, 2015; McGarigal et al., 2012).

2.3.4. LULC change intensity and landscape fragmentation correlation

The Pearson correlation test is a statistical method used to assess the linear relationship between landscape-level LULC change intensity (St) and landscape metrics. This test can provide valuable insights into how changes in LULC impact landscape fragmentation.

To conduct a Pearson correlation analysis, LULC change intensity at the interval level (*St*) and landscape metrics were calculated for each time period (1990–2000, 2000–2010, and 2010–2020) across all functional zones. The calculated variables were imported into RStudio 2024.09 for analysis. Pearson correlation coefficients were computed to quantify the linear relationships between LULC change intensity and each landscape metric, as well as among the landscape metrics themselves.

Pearson's correlation coefficient (r_{xy}) is defined as:

$$r_{xy} = \frac{n\sum x_i y_i - \sum x_i \sum y_i}{\sqrt{n\sum x_i^2 - (\sum x_i)^2}\sqrt{n\sum y_i^2 - (\sum y_i)^2}} \quad (7)$$

Where: n is the sample size; x_i, *yi* are the individual sample points indexed with *i*.

This coefficient ranges from -1 to +1. Values close to 1 indicate a strong positive correlation, meaning that fragmentation also increases as land change intensity increases. Values close to -1 indicate a strong negative correlation, meaning that as one variable increases, the other decreases. Values around 0 suggest no linear relationship between the variables.

3. Results

3.1. Accuracy assessment

Based on the summarized results of the LULC classification accuracy (Table A.2), the producer and user accuracy values for evergreen broadleaf forest, barren land, grassland/herbaceous vegetation, bamboo area, and open water were predominantly above 85%. These values significantly surpassed those of the remaining classes, such as plantation land, low-developed areas, rice paddies, woody crops, and other croplands.

Overall accuracy values of 81.60%, 83.87%, 84.40%, and 85.33%, along with κ values of 0.80, 0.82, 0.83, and 0.84, were obtained for the LULC classifications of 1990, 2000, 2010, and 2020, respectively. These results indicate a reasonably good agreement between the classified classes and the ground truth, as reported by Congalton (1991). Although the overall accuracy and κ values were slightly below the minimum accuracy requirements of 85–90 percent recommended by Anderson (1976), they still demonstrate good consistency and significant agreement (Fung & LeDrew, 2008; Mao & Wang, 2012).

3.2. LULC change during 1990–2020

The LULC classification results from 1990, 2000, 2010, and 2020 are shown in Table A.3, while the distribution of the 13 LULC types over these years is illustrated in Fig. 3 and Fig. A.1. As depicted, evergreen broadleaf forest consistently accounts for the most significant proportion of land, ranging from 46% to 55.6%. This is followed by plantation land, comprising 16.4% to 28.4%, and bamboo area, which covers 6.4% to 10.5%. Other croplands constitute 6.3% to 9.3%, grassland/herbaceous vegetation accounts for 3.6% to 6%, woody crops cover 3.1% to 4.7%, and rice paddies make up 1.3% to 2.4%.

In contrast, the remaining LULC types highly developed areas, low-developed areas, barren land, scrub/shrub, open water, and aquaculture - collectively represent a tiny fraction of the total area of the WNABR, each accounting for less than 1%.

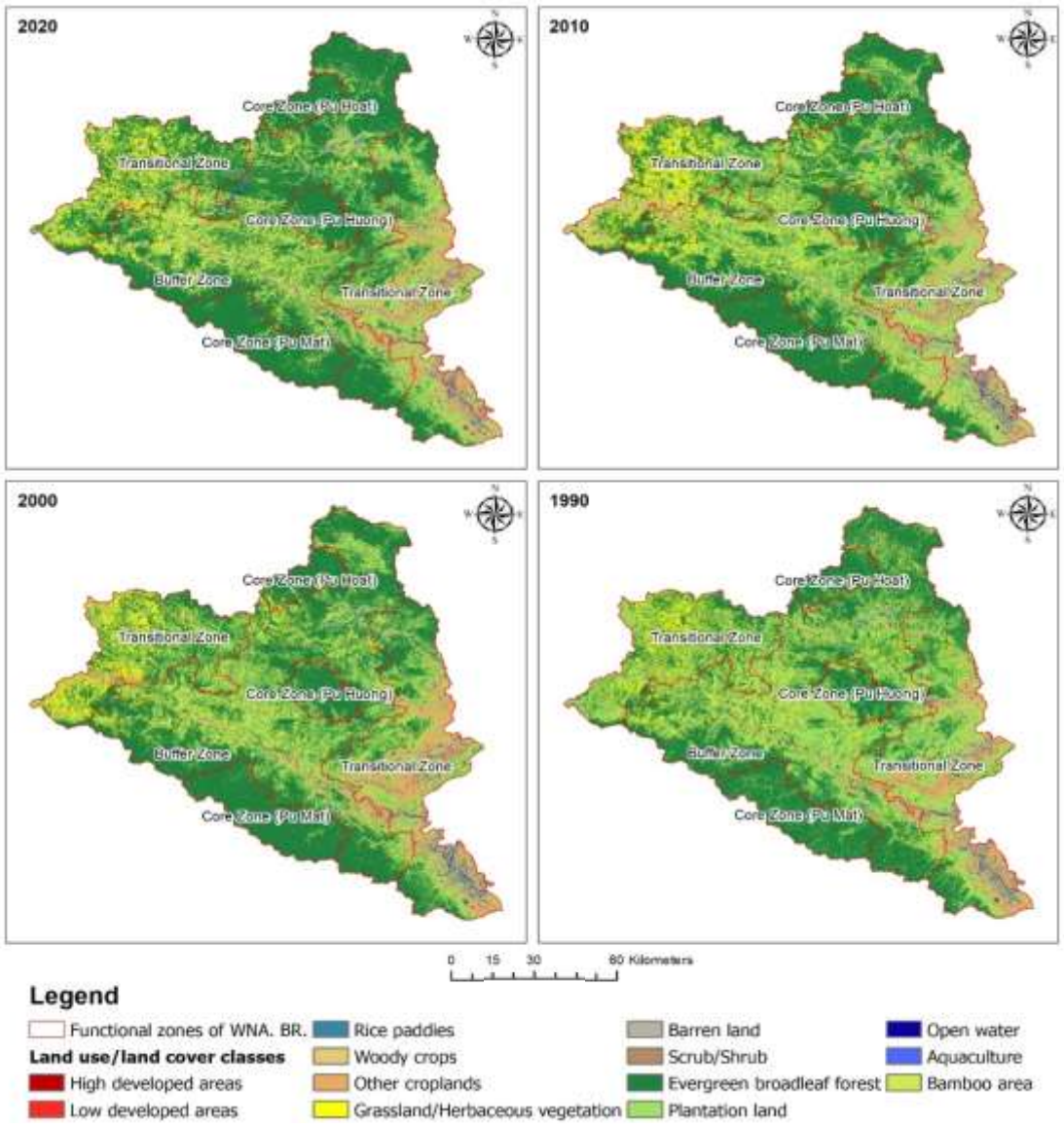

Figure 3. LULC classification of the Western Nghe An Biosphere Reserve

In terms of the extent of functional zones in the WNABR, the buffer zone covers the most significant area (616,698 hectares), followed by the transition zone (507,703 hectares). Pu Mat National Park (core zone) spans 95,156 hectares, while Pu Huong Natural Reserve (core zone) and Pu Hoat Natural Reserve (core zone) cover 36,925 hectares and 41,972 hectares, respectively.

Evergreen broadleaf forest and plantation land constitute the largest share of the structure of all functional zones. In the core areas, 70.8% to 97.1% is covered by evergreen broadleaf forest, 0.3% to 22.8% is plantation land, with the remaining LULC types accounting for a tiny proportion. In other functional zones, evergreen broadleaf forests and plantation land remain dominant,

though their proportions are lower than in the core zones.

In the buffer zone, evergreen broadleaf forest areas range from 49% to 60.5%, plantation land ranges from 11.2% to 28.1%, and bamboo areas range from 9.5% to 16.9%. Agricultural systems, such as paddy fields, woody crops, and other croplands, each account for 3–5%. The proportion of evergreen broadleaf forest in the transition zone is lower than in the buffer and core zones (29–36.8%). Conversely, the proportion of plantation land and agricultural cropping systems, such as woody crops and other croplands, is higher in the buffer and core zones than in the buffer and core zones.

This trend indicates that human influence gradually increases from the core zones to the buffer and transition zones through the expansion of residential and productive land. This transformation shifts natural forest ecosystems into degraded systems (e.g., bamboo areas, grasslands, barren land), agricultural systems, and settlements. This progression aligns with the operational management protocols permitted in UNESCO-regulated Biosphere Reserves since the WNABR was first designated as a Biosphere Reserve in 2007.

Between 1990 and 2020, there was an observed increase in highly developed areas, low-developed areas, woody crops, barren land, evergreen broadleaf forests, open water, aquaculture, and bamboo areas. Notably, during the periods 1990–2000, 2000–2010, and 2010–2020, there was a continuous rise in highly developed areas, low-developed areas, and bamboo areas. Conversely, plantation land, scrub/shrub, grassland/herbaceous vegetation, other croplands, and rice paddies declined during these periods.

From 1990 to 2000 and from 2010 to 2020, plantation land experienced significant declines. Similarly, the area covered by scrub/shrub steadily decreased between 2000 and 2020. Although the decline in rice paddies' area was primarily observed between 2010 and 2020, there was an overall reduction throughout the entire 1990–2020 period (Fig. A.1 and Fig. A.2).

The most significant net change in LULC over the period 1990–2020 was observed in highly developed areas, with an average net change of 122.72 percent, and in low-developed regions, with an average net change of 221.75 percent. These were followed by aquaculture (7.91 percent/year), barren land (4.89 percent/year), and bamboo areas (2.09 percent/year). Conversely, scrub/shrub (-2.19%/year), plantation land (-1.40%/year), grassland/herbaceous vegetation (-0.98%/year), and rice paddies (-0.84%/year) experienced the greatest declines (Table A.3).

Figure A.2 and Fig. A.3 illustrate the dynamic conversions among different LULC types. Notably, most plantation land The lost between 1990 and 2020 was converted to evergreen broadleaf forest, woody crops, and grassland/herbaceous vegetation. Concurrently, plantation forests, woody crops, bamboo areas, and grasslands/herbaceous vegetation were the primary contributors to the decline in evergreen broadleaf forest area. Additionally, plantation land, other croplands, scrub/shrub, and grassland/herbaceous vegetation were the primary sources of the increase in woody crops, highly developed areas, and low-developed areas.

3.3. LULC intensity analysis

3.3.1. LULC change intensity at the interval level

Between 1990 and 2000, the annual land-use change intensity was 4.38%, exceeding the uniform intensity of 4.11%, suggesting rapid land-use change during this period (Fig. A. 6a). However, from 2000 to 2010, and from 2010 to 2020, the annual land-use change intensities were 4.10% and 3.84%, respectively, both below the average value. This indicates that land use changes slowed during these latter periods.

Analyzing the functional zones, it is evident that the annual land-use change intensity in the transition and buffer zones frequently exceeds the average uniform intensity of 4.1% (Fig. 4). This suggests that land use changes are occurring more rapidly in these zones. Conversely, the land use change intensity values for the three core zones are consistently lower than the average and have gradually declined since 2000. This trend indicates slower land-use changes in these areas, reflecting the effectiveness of conservation efforts since the WNABR was first recognized in 2007.

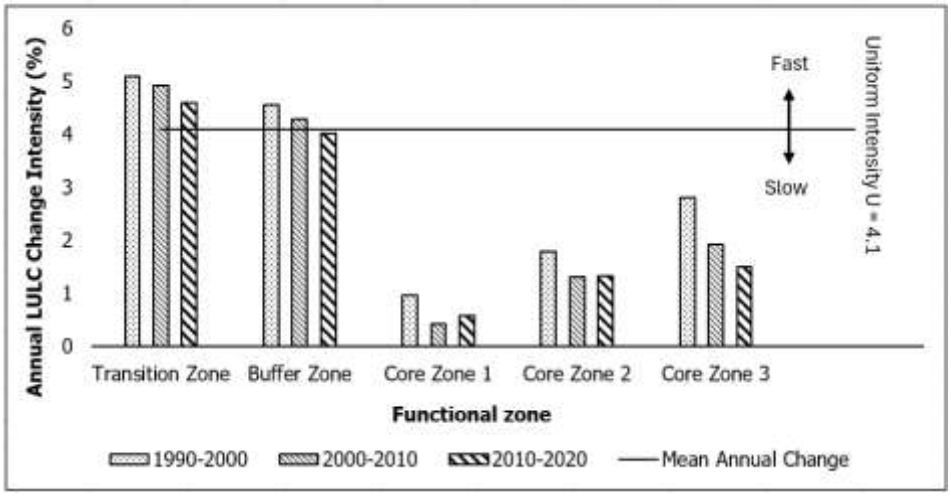

Figure 4. LULC change intensity at the interval level is calculated for each functional zone

3.3.2. LULC change intensity at category level

According to the land use intensity change analysis of WNABR at the category level (Fig. A.6 b, c, d), the values for evergreen broadleaf forest, open water, other croplands, and rice paddies are generally below or around the uniform intensity value (0.41), indicating that these land use types are relatively dormant. In contrast, the values for the remaining land use types exceed The average, signifying that these types are active. Specifically, bamboo areas, grassland/herbaceous vegetation, barren land, highly developed areas, low-developed areas, scrub/shrub, and woody crops exhibit the highest change-intensity values, making them the most dynamic land cover types undergoing significant transformations between 1990 and 2020.

3.4. Landscape pattern and landscape fragmentation change

The results of the landscape metric analysis, presented in Table 1, reveal several key trends. The metrics ED, PRFAC, NP, PD, LSI, SHDI, and SHEI all slightly declined over time. Conversely, the AI index gradually increased to 80. This suggests that, by 2020, the WNABR landscape was generally less fragmented than in 1990. The aggregation of landscape fragments has increased, while the overall landscape diversity has gradually declined. The relatively stable metrics indicate that landscape aggregation and connectedness are occurring slowly.

Table 1. Calculation results of landscape metrics at landscape level from 1990 to 2020

Group	Landscape Metric	1990	2000	2010	2020
Area-Edge	LPI	16.35	18.57	17.55	17.04
	ED	190.69	174.52	165.91	134.56
Shape	SHAPE_MN	1.2	1.2	1.2	1.22
	FRAC_MN	1.04	1.04	1.04	1.04
	PAFRAC	1.55	1.54	1.53	1.51
Aggregation	NP	955727	895181	784244	592475
	PD	73.59	68.93	60.39	45.62
	LSI	545.39	499.34	474.82	385.51
	COHESION	99.64	99.61	99.43	99.55
	AI	72.08	74.44	75.7	80.09
Diversity	PR	12	12	12	12
	SHDI	1.48	1.5	1.53	1.42
	SHEI	0.6	0.6	0.62	0.57

While landscape complexity has decreased, it remains relatively high, as evidenced by PARFAC values consistently above 1.5. Similar trends are observed across all functional zones of the WNABR. Decreases in the PRFAC, NP, PD, LSI, SHDI, and SHEI indices were noted in the core, buffer, and transition zones (Table A.4). The AI index increased across all functional zones, approaching 100 in the core areas. This illustrates a reduction in landscape fragmentation at the landscape level, with core areas exhibiting nearly solid and less fragmented landscapes.

Further analysis of Table A.4 indicates that the buffer and transition zones have substantially lower LPI index values compared to the core zones. Conversely, the ED, NP, PD, LSI, SHDI, and SHEI indices in the core zones are lower than those in the other two zones. The landscape shape indices (SHAPE_MN, FRAC_MN, and PARFAC) show slight variation among zones, suggesting that although the buffer and transition zones exhibit significantly higher landscape fragmentation, patch complexity remains consistent across all functional zones.

Figure A.5 presents the findings of the class-level analysis of landscape metrics. There is a slight variation in the shape and complexity of LULC types, as evidenced by landscape shape indices such as PARFAC, SHAPE_MN, and FRAC_MN. The PLAN, LPI, ED, AI, and COHESION indices for evergreen broadleaf forests are the highest among the landscape classes and have steadily increased from 1990 to 2020. This indicates that evergreen broadleaf forests experience the least fragmentation, with the largest patch areas and the fewest fragments. Similarly, plantation land and bamboo areas are more extensive and less fragmented compared to other landscape classes, except for evergreen broadleaf forests.

The LSI, NP, PD, AI, and LSI indices are high in woody crops, other croplands, and grassland/herbaceous vegetation, whereas PLAND, LPI, and ED indices are low. This suggests that these classes consist of small patches but exhibit good landscape aggregation. Highly developed areas, low-developed areas, barren land, scrub/shrub, rice paddies, and open water have low values in PLAN, LPI, ED, NP, PD, LSI, and AI metrics, indicating numerous small, dispersed areas. However, PLAN, LPI, ED, NP, PD, LSI, and AI metrics tend to increase in both high- and low-developed area classes, suggesting that these LULC types are growing and becoming more aggregated over time.

The SHAPE_MN, FRAC_MN, and PARFAC_MN indices show little variation across landscape classes and functional zones, indicating minimal differences in complexity between the landscape layers inside and outside the core areas. Evergreen broadleaf forests have the highest PLAN, AI, and COHESION values among all landscape classes. This PLAN value is also the highest in the core areas. It decreases progressively in the buffer and transition zones, indicating that the evergreen broadleaf forest is well protected in the core areas, while the outer layers are more fragmented.

In Pu Huong Natural Reserve (core zone) and the transition zone, plantation land has the highest PLAN index. PLAN is at a low

average level in other regions, suggesting that plantation land is more fragmented than evergreen broadleaf forest. These metrics collectively indicate that buffer and transition zones exhibit significantly greater landscape fragmentation than core zones, even though patch complexity remains consistent across functional zones.

3.5. LULC change intensity, change, and landscape fragmentation metrics correlation

The Pearson correlation test results indicate that land change intensity has a significant positive correlation with NP (number of patches) and no clear correlation with other variables (Fig. 5). The correlation coefficient between Change Intensity and NP is 0.59, suggesting a strong relationship between LULC change intensity and the number of patches.

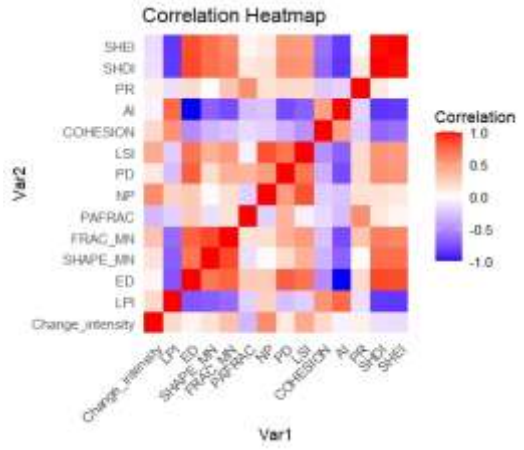

Figure 5. Correlation heatmap of Change intensity and Landscape metrics

Correlation Among Landscape Metrics:

- Area-Edge Metrics: LPI exhibits a strong negative correlation with ED, SHAPE_MN, FRAC_MN, SHDI, and SHEI. This implies that as LPI decreases, the degree of fragmentation, landscape diversity, and complexity of patch shapes increase. ED has a strong negative correlation with LPI and AI, and a strong positive correlation with SHAPE_MN, FRAC_MN, PD, LSI, SHDI, and SHEI. This indicates that the landscape becomes more fragmented, diverse, and complex as edge density increases.

- Shape Metrics: SHAPE_MN and FRAC_MN are positively correlated with each other but do not correlate with PARFAC. Both SHAPE_MN and FRAC_MN show strong negative correlations with LPI and AI, and strong positive correlations with ED, SHDI, and SHEI. This suggests that fragmentation, diversity, and edge density also increase as landscape complexity rises.

- Aggregation Metrics: NP is the only metric positively correlated with LULC change intensity. LSI shows positive correlations with NP, PD, and ED and a strong negative correlation with AI. PD is positively correlated with ED, LSI, SHDI, and SHEI, and negatively correlated with COHESION. COHESION is positively correlated with LPI and negatively correlated with SHDI and SHEI. AI is strongly negatively correlated with ED, SHAPE_MN, FRAC_MN, PD, LSI, SHDI, and SHEI.

- Diversity Metrics: SHDI and SHEI are strongly positively correlated with each other and show no correlation with PR and LULC change intensity. This indicates that increased landscape fragmentation does not necessarily correspond to higher patch richness or change intensity. Additionally, SHDI and SHEI do not have clear correlations with PARFAC and NP, but are strongly positively correlated with SHAPE_MN and FRAC_MN.

This analysis reveals the complex interactions between LULC change intensity and various landscape metrics, providing insights into how land-use changes impact landscape fragmentation and diversity.

5. Discussions

5.1. The use of LULC change intensity analysis and landscape metrics

The correlation analysis of landscape metrics in the study area from 1990 to 2020

indicates that most are interrelated. This aligns with the findings of Hargis et al. (1998), who observed that many metrics were highly correlated. Based on the correlation coefficients among variables, landscape metrics such as LPI, ED, SHAPE_MN, FRAC_MN, NP, AI, and SHDI can be employed to gauge the intensity and complexity of landscape fragmentation. This approach is consistent with previous studies that primarily used metrics like Mean Patch Size (MPS), Number of Patches (NP), Total Edge (TE), Edge Density (ED), Largest Patch Index (LPI), Aggregation Index (AI), and Shannon's Diversity Index (SHDI) to measure landscape fragmentation (Southworth et al., 2002; Uuemaa et al., 2009).

The analysis results reveal that the SHDI and SHEI indices are strongly positively correlated with each other and significantly correlated with other landscape metrics, including AI, COHESION, LPI (negative correlation), ED, SHAPE_MN, FRAC_MN, LSI, and PD (positive correlation). Therefore, the SHDI/SHEI indices can be used as composite indicators to measure the extent of fragmentation and the shape complexity of landscape patches. Fletcher et al. (2023) suggest that SHDI is particularly useful at the landscape scale, where it helps identify patterns of biodiversity loss due to fragmentation. Numerous studies have used the SHDI metric to assess species richness and evenness (Riva & Fahrig, 2023) and to quantify changes in ecosystem service value (ESV) (Biswas et al., 2023), thereby aiding in managing landscapes to support both biodiversity and ecosystem functions.

In this study, the Number of Patches (NP) is the only metric with a strong positive correlation to LULC change intensity. This finding suggests that NP is particularly sensitive to land use changes in the study area. Therefore, NP can effectively measure and validate LULC change intensity. An increase in NP indicates higher landscape fragmentation, which correlates with increased LULC change intensity, and vice versa. No studies have investigated the relationship between LULC change intensity values and landscape metrics. Thus, further research on these correlations is essential to enhance our understanding of how increased land-use intensity affects landscape fragmentation. This knowledge can then inform the development of effective strategies and interventions.

While landscape metrics offer valuable insights into fragmentation, they do have limitations (Uuemaa et al., 2009). The complexity of landscapes and variability in data quality can affect the accuracy of these metrics (Frazier & Kedron, 2017; Newman et al., 2019). Additionally, the choice of metrics and scales can influence the interpretation of fragmentation patterns (Fletcher Jr. et al., 2023). Therefore, it is crucial to integrate multiple metrics, including LULC change intensity, for a comprehensive understanding of landscape fragmentation and its driving forces.

5.2. The implication for biodiversity conservation

The LULC change and landscape fragmentation analysis revealed an expansion of an evergreen broadleaf forest assemblage throughout the WNABR and its functional zones. Moreover, the increase in area and reduction in fragmentation of bamboo areas and barren land suggest that, despite being degraded ecosystems, these LULC types can maintain connectivity and potentially be restored to strengthen habitat linkage.

The analysis identified the most extensive and least fragmented evergreen broadleaf forest in the WNABR's three core areas. Beyond these core zones, evergreen broadleaf forest becomes increasingly fragmented and replaced by plantation land, agricultural ecosystems (e.g., rice paddies, woody crops,

other croplands), degraded forest types (e.g., barren land, bamboo areas), and human settlements (e.g., high and low developed areas). Apart from plantation areas and evergreen broadleaf forests, other LULC types are typically small and fragmented.

The gradient of landscape naturalness and fragmentation in the WNABR decreases progressively from the core areas to the buffer and transition zones, aligning with the integrity value of the forest landscape (Grantham et al., 2020). The forest landscape integrity value reaches its peak in the three core zones and gradually diminishes in the buffer and transition zones due to increased human presence and economic activities. Based on the island biogeography theory of MacArthur & Wilson (2001), the three core areas of the WNABR act as biodiversity hotspots, preserving and enhancing biodiversity in the region. In addition to protecting these core areas, it is essential for Nghe An Province to assess and restore natural and semi-natural forests, or to reforest degraded systems (e.g., bamboo area, grassland/herbaceous vegetation, scrub/shrub, and barren land), while limiting the spread of human-dominated LULC types. These measures would help create biodiversity corridors and strengthen ecological connectivity networks, thus contributing to biodiversity conservation Gurrutxaga et al., 2010; Hoctor et al., 2000).

Landscape fragmentation and habitat loss significantly impact biodiversity conservation and the functioning of natural ecosystems (Fahrig, 2003; Haddad et al., 2015). Fragmentation can lead to persistent, damaging, and often unpredictable outcomes (Haddad et al., 2015), resulting in loss of connectivity and increased risk of species extinction, especially in the context of climate change (Brooks et al., 2002; Mantyka-Pringle et al., 2012). According to Phung Van Khoa et al. (2023), LULC change is the primary threat causing the decline of gibbons (*Hylobatidae*) in the WNABR. Unfortunately, so far, there have been no in-depth studies on the relationship between land-use change and biodiversity change in WNABR. This issue requires further research to develop biodiversity conservation solutions based on effective land-use management. In addition, the research area is characterized by complex natural conditions and is inhabited by various ethnic groups, each with distinct economic, cultural, and livelihood conditions. Consequently, it is imperative to conduct comprehensive research into the driving forces of land-use change and their trends to develop appropriate solutions.

5.3. Uncertainties and limitations of the research

This study utilizes large-scale LULC level-2 data, comprising 18 different classes of secondarily dominant LULC, with a spatial resolution of 30 m for all of Vietnam and an overall accuracy of 75–85 percent (Phan et al., 2021). Although the accuracy assessment results for the WNABR are pretty good (overall accuracy: 81.60–85.33%; κ values: 0.80–0.84), they remain slightly below the threshold recommended by Anderson (1976). The user and producer accuracy values for certain LULC types, such as plantation land (in 1990), low-developed areas, woody crops, other croplands, and scrub/shrub, hover around 70 percent.

This reduced accuracy is attributed to the separation of these level-2 LULC types from ten level-1 LULC types, which have an overall accuracy of 86–92 percent (water, urban/built-up, rice, other crops, grass/shrub, woody crops/orchards, barren, evergreen forest, deciduous forest, plantation forest, aquaculture) (Jaxa et al., 2021; Phan et al., 2021). Increasing the number of classification classes (LULC types) generally decreases classification accuracy (Thinh et al., 2019).

These LULC types often consist of small, scattered patches commonly found under forest canopies in mountainous areas. They are relatively difficult to distinguish from larger objects, such as forests, bamboo areas, shrubs, and woody crops, in classifying medium-resolution satellite images such as Landsat and Sentinel (Espinoza et al., 2023; Yang & Song, 2023).

Therefore, it is necessary to use high-resolution imagery data for LULC classification to more accurately distinguish anthropogenic LULC types, such as rice paddies, cropland, urban settlements, and rural settlements in mountainous regions.

6. Conclusions

The WNABR has undergone significant changes in land use and land cover (LULC) over 30 years, from 1990 to 2020. Major LULC trends include increases in highly developed areas, less developed regions, woody crops, barren land, and open water, aquaculture, and bamboo areas. In contrast, plantation land, scrub/shrub, grassland/herbaceous vegetation, other croplands, and rice paddies have declined. Nevertheless, evergreen broadleaf forest remains dominant, covering 55% of the WNABR.

Land change intensity peaked from 1990 to 2000 and gradually decreased from 2000 to 2020. The buffer and transition zones experienced greater land change intensity than the core zone. Evergreen broadleaf forests, open water, other croplands, and rice paddies exhibited lower land change intensity than other types. Despite ongoing LULC conversions, there is a general trend of decreasing fragmentation within the WNABR. Evergreen broadleaf forest and plantation land comprise large, less fragmented patches, while the remaining LULC types are typically fragmented into small, scattered patches. Moving from the core zone to the buffer and transition zones, ecosystem naturalness gradually decreases, and LULC fragmentation increases due to human presence and activities. Land change intensity has a significant positive linear relationship with the number of patches (NP). Therefore, the NP index is reliable for measuring and validating land change intensity.

LULC changes and landscape fragmentation contribute to biodiversity loss and species extinction. WNABR comprises three distinct core zones. For effective biodiversity conservation, it is vital to preserve the ecological integrity of these core zones and enhance habitat connectivity between them. This can be achieved by planning landscape corridors within the buffer and transition zones, thereby linking the core zones together. Nghe An Province needs to identify and assess biodiversity corridors and strengthen ecological networks to support biological conservation in the WNABR. However, it is essential to conduct in-depth studies to elucidate the causes of land-use change and their impacts on the biodiversity of the study area, specifically identifying which species are affected and how. This will enable the development of effective conservation strategies and solutions that are integrated with economic development and livelihood improvement for the local communities within the biosphere reserve.

This study introduces a comprehensive framework for investigating the relationships among land-use change, land-use change intensity, and landscape fragmentation. It elucidates the underlying mechanisms and provides methodologies for effectively monitoring LULC change and landscape fragmentation in the biosphere reserve. The findings from this analysis will help refine land-use planning processes, ensuring they align with biodiversity conservation strategies in areas of high ecological significance.

Acknowledgements

The scientific project supported this research, No. QG.20.24, funded by the Vietnam National University (VNU), Hanoi.

References

Aldwaik S.Z., Pontius R.G., 2012. Intensity analysis to unify measurements of size and stationarity of land changes by interval, category, and transition. Landscape and Urban Planning, 106(1), 103–114. https://doi.org/10.1016/j.landurbplan.2012.02.010.

Amini Parsa V., Yavari A., Nejadi A., 2016. Spatio-temporal analysis of land use/land cover pattern changes in Arasbaran Biosphere Reserve: Iran. Modeling Earth Systems and Environment, 2(4), 1–13. https://doi.org/10.1007/s40808-016-0251-5.

Anderson J.R., 1976. A land use and land cover classification system for use with remote sensor data, 964. US Government Printing Office. https://doi.org/10.3133/pp964.

Anteneh Y., Stellmacher T., Zeleke G., Mekuria W., Gebremariam E., 2018. Dynamics of land change: Insights from a three-level intensity analysis of the Legedadie-Dire catchments, Ethiopia. Environmental Monitoring and Assessment, 190(5), 309. https://doi.org/10.1007/s10661-018-6688-1.

Batisse M., 1982. The biosphere reserve: A tool for environmental conservation and management. Environmental Conservation, 9(2), 101–111. https://doi.org/10.1017/S0376892900019937.

Batisse M., 1997. Biosphere reserves: A challenge for biodiversity conservation & regional development. Environment: Science and Policy for Sustainable Development, 39(5), 6–33. https://doi.org/10.1080/00139159709603644.

Biswas G., Sengupta A., Alfaisal F.M., Alam S., Alharbi R.S., Jeon B.-H., 2023. Evaluating the effects of landscape fragmentation on ecosystem services: A three-decade perspective. Ecological Informatics, 77, 102283. https://doi.org/10.1016/j.ecoinf.2023.102283.

Brooks T.M., et al., 2002. Habitat loss and extinction in the hotspots of biodiversity. Conservation Biology, 16(4), 909–923. https://doi.org/10.1046/j.1523-1739.2002.00530.x.

Clerici N., Bodini A., Eva H., Grégoire J.-M., Dulieu D., Paolini C., 2007. Increased isolation of two Biosphere Reserves and surrounding protected areas (WAP ecological complex, West Africa). Journal for Nature Conservation, 15(1), 26–40. https://doi.org/10.1016/j.jnc.2006.08.003.

Congalton R.G., 1991. A review of assessing the accuracy of classifications of remotely sensed data. Remote Sensing of Environment, 37(1), 35–46. https://doi.org/10.1016/0034-4257(91)90048-B.

Do A.N.T., Tran H.D., Ashley M., Nguyen A.T., 2022. Monitoring landscape fragmentation and aboveground biomass estimation in Can Gio Mangrove Biosphere Reserve over the past 20 years. Ecological Informatics, 70, 101743. https://doi.org/10.1016/j.ecoinf.2022.101743.

Duan X., Chen Y., Wang L., Zheng G., Liang T., 2023. The impact of land use and land cover changes on the landscape pattern and ecosystem service value in Sanjiangyuan region of the Qinghai-Tibet Plateau. Journal of Environmental Management, 325, 116539. https://doi.org/10.1016/j.jenvman.2022.116539.

Espinoza V., Booth L.A., Viers J.H., 2023. Land Use Misclassification Results in Water Use, Economic Value, and GHG Emission Discrepancies in California's High-Intensity Agriculture Region. Sustainability, 15(8), 6829. https://doi.org/10.3390/su15086829.

Ettehadi Osgouei P., Sertel E., Kabaday M.E., 2022. Integrated usage of historical geospatial data and modern satellite images reveal long-term land use/cover changes in Bursa/Turkey, 1858–2020. Scientific Reports, 12(1), 9077. https://doi.org/10.1038/s41598-022-11396-1.

Fahrig L., 2003. Effects of habitat fragmentation on biodiversity. Annual Review of Ecology, Evolution, and Systematics, 34(1), 487–515. https://doi.org/10.1146/annurev.ecolsys.34.011802.132419.

Figueroa F., Sánchez-Cordero V., Meave J.A., Trejo I., 2009. Socioeconomic context of land use and land cover change in Mexican biosphere reserves. Environmental Conservation, 36(3), 180–191. https://doi.org/10.1017/S0376892909990221.

Fischer J., Lindenmayer D.B., 2007. Landscape modification and habitat fragmentation: A synthesis.

Global Ecology and Biogeography, 16(3), 265–280. https://doi.org/10.1111/j.1466-8238.2007.00287.x.

Fletcher Jr. R.J., Betts M.G., Damschen E.I., Hefley T.J., Hightower J., Smith T.A.H., Fortin M.-J., Haddad N.M., 2023. Addressing the problem of scale that emerges with habitat fragmentation. Global Ecology and Biogeography, 32(6), 828–841. https://doi.org/10.1111/geb.13658.

Foody G.M., 2020. Explaining the unsuitability of the kappa coefficient in the assessment and comparison of the accuracy of thematic maps obtained by image classification. Remote Sensing of Environment, 239, 111630. https://doi.org/10.1016/j.rse.2019.111630.

Frazier A.E., Kedron P., 2017. Landscape Metrics: Past Progress and Future Directions. Current Landscape Ecology Reports, 2(3), 63–72. https://doi.org/10.1007/s40823-017-0026-0.

Fung T., Le Drew E., 2008. The Determination of Optimal Threshold Levels for Change Detection Using Various Accuracy Indices. https://www.semanticscholar.org/paper/The-Determination-of-Optimal-Threshold-Levels-for-Fung-LeDrew/da6c9f9e93c41237f95f7ca7216ba4807d4bbda2.

Grantham H.S., et al., 2020. Anthropogenic modification of forests means only 40% of remaining forests have high ecosystem integrity. Nature Communications, 11(1), 5978. https://doi.org/10.1038/s41467-020-19493-3.

Gurrutxaga M., Lozano P.J., del Barrio G., 2010. GIS-based approach for incorporating the connectivity of ecological networks into regional planning. Journal for Nature Conservation, 18(4), 318–326. https://doi.org/10.1016/j.jnc.2010.01.005.

Hargis C.D., Bissonette J.A., David J.L., 1998. The behavior of landscape metrics commonly used in the study of habitat fragmentation. Landscape Ecology, 13(3), 167–186. https://doi.org/10.1023/A:1007965018633.

Hilton-Taylor C., Brackett D., 2000. 2000 IUCN red list of threatened species. IUCN, Gland, Switzerland and Cambridge, UK.

Hoctor T.S., Carr M.H., Zwick P.D., 2000. Identifying a linked reserve system using a regional landscape approach: The Florida ecological network. Conservation Biology, 14(4), 984–1000. https://doi.org/10.1046/j.1523-1739.2000.99075.x.

Hu Y., Batunacun Zhen L., Zhuang D., 2019. Assessment of Land-Use and Land-Cover Change in Guangxi, China. Scientific Reports, 9(1), 2189. https://doi.org/10.1038/s41598-019-38487-w.

Jxa, Eorc, Alos, 2021. Annual Land-Use and Land-Cover Maps across Mainland Vietnam from 1990 to 2020 (Released in September 2021/Version 21.09). Annual Land-Use and Land-Cover Maps across Mainland Vietnam from 1990 to 2020 (Released in September 2021/Version 21.09). https://www.eorc.jaxa.jp/ALOS/dataset/lulc_e.htm.

Kušová D., Těšitel J., Matějka K., Bartoš M., 2008. Biosphere reserves-An attempt to form sustainable landscapes: A case study of three biosphere reserves in the Czech Republic. Landscape and Urban Planning, 84(1), 38–51. https://doi.org/10.1016/j.landurbplan.2007.06.006.

MacArthur R.H., Wilson E.O., 2001. The theory of island biogeography. Princeton University Press. https://doi.org/10.2307/j.ctt19cc1t2.

Mantyka-pringle C.S., Martin T.G., Rhodes J.R., 2012. Interactions between climate and habitat loss effects on biodiversity: A systematic review and meta-analysis. Global Change Biology, 18(4), 1239–1252. https://doi.org/10.1111/j.1365-2486.2011.02593.x.

Mao W., Wang F.-Y., 2012. Chapter 4 Forecasting Group Behavior via Probabilistic Plan Inference. In W. Mao & F.-Y. Wang (Eds.), New Advances in Intelligence and Security Informatics. Academic Press, 33–44. https://doi.org/10.1016/B978-0-12-397200-2.00004-X.

McAlpine C.A., Eyre T.J., 2002. Testing landscape metrics as indicators of habitat loss and fragmentation in continuous eucalypt forests (Queensland, Australia). Landscape Ecology, 17(8), 711–728. https://doi.org/10.1023/A:1022902907827.

McGarigal K., 2013. Landscape Pattern Metrics. In Encyclopedia of Environmetrics. John Wiley & Sons, Ltd. https://doi.org/10.1002/9780470057339.val006.pub2

McGarigal K., 2015. FRAGSTATS help. University of Massachusetts: Amherst, MA, USA, 182. http://www.umass.edu/landeco/research/fragstats/documents/fragstats.help.4.2.pdf

Michel O.O., Ying Y., Wenyi F., Chen C., Kaiko K.S., 2021. Examining Land Use/Land Cover Change and Its Prediction Based on a Multilayer Perceptron

Markov Approach in the Luki Biosphere Reserve, Democratic Republic of Congo. Sustainability, 13(12), 6898. https://doi.org/10.3390/su13126898.

Newman E.A., Kennedy M.C., Falk D.A., McKenzie D., 2019. Scaling and Complexity in Landscape Ecology. Frontiers in Ecology and Evolution, 7, 293. https://doi.org/10.3389/fevo.2019.00293.

Nghe An People Committee, 2017. 10-year assessment report of the Western Nghe An Biosphere Reserve period 2007–2017.

Nghe An People Committee, 2021. Nghe An statistical yearbook 2020. Statistical Publisher.

Nguyen Tien Lam, 2016. Handbook of the Western Nghe An Biosphere Reserve.

Phan D.C., Trung T.H., Truong V.T., Sasagawa T., Vu T.P.T., Bui D.T., Hayashi M., Tadono T., Nasahara K.N., 2021. First comprehensive quantification of annual land use/cover from 1990 to 2020 across mainland Vietnam. Scientific Reports, 11(1), 9979. https://doi.org/10.1038/s41598-021-89034-5.

Phung K.V., Tran D.V., Dong H.T., Luu V.Q., Bui V.B., Vu T.T., 2023. Changes in suitable habitat for the critically endangered Northern white-cheeked gibbon (Nomascus leucogenys) in the Western Nghe An Biosphere Reserve, Vietnam: Implication for conservation. Nature Conservation, 51, 167–188. https://doi.org/10.3897/natureconservation.51.90373

Reed M.G., 2019. The contributions of UNESCO Man and Biosphere Programme and biosphere reserves to the practice of sustainability science. Sustainability Science, 14(3), 809–821. https://doi.org/10.1007/s11625-018-0603-0.

Riva F., Fahrig L., 2023. Landscape-scale habitat fragmentation is positively related to biodiversity, despite patch-scale ecosystem decay. Ecology Letters, 26(2), 268–277. https://doi.org/10.1111/ele.14145.

Rivas-Tabares D., Tarquis A.M., De Miguel Á., Gobin A., Willaarts B., 2022. Enhancing LULC scenarios impact assessment in hydrological dynamics using participatory mapping protocols in semiarid regions. Science of the Total Environment, 803, 149906. https://doi.org/10.1016/j.scitotenv.2021.149906.

Rosenfield G.H., Fitzpatrick-Lins K., 1986. A coefficient of agreement as a measure of thematic classification accuracy. Photogrammetric Engineering and Remote Sensing, 52(2), 223–227. https://pubs.usgs.gov/publication/70014667.

Southworth J., Nagendra H., Tucker C., 2002. Fragmentation of a Landscape: Incorporating landscape metrics into satellite analyses of land-cover change. Landscape Research, 27(3), 253–269. https://doi.org/10.1080/01426390220149511.

Sun L., Yu H., Sun M., Wang Y., 2023. Coupled impacts of climate and land use changes on regional ecosystem services. Journal of Environmental Management, 326, 116753. https://doi.org/10.1016/j.jenvman.2022.116753.

Thinh T.V., Duong P.C., Nasahara K.N., Tadono T., 2019. How Does Land Use/Land Cover Map's Accuracy Depend on Number of Classification Classes? Sola, 15, 28–31. https://doi.org/10.2151/sola.2019-006.

UNESCO, 2018. Western Nghe An Biosphere Reserve, Viet Nam. UNESCO. https://en.unesco.org/biosphere/aspac/western-nghe-an.

UNESCO, 2023a. Biosphere reserves in Asia and the Pacific. UNESCO. https://en.unesco.org/biosphere/aspac.

UNESCO, 2023b. World Network of Biosphere Reserves. https://en.unesco.org/biosphere/wnbr.

Uuemaa E., Antrop M., Roosaare J., Marja R., Mander Ü., 2009. Landscape metrics and indices: an overview of their use in landscape research. Living Reviews in Landscape Research, 3(1), 1–28. https://doi.org/10.12942/lrlr-2009-1.

Van Cuong C., Dart P., Hockings M., 2017. Biosphere reserves: Attributes for success. Journal of Environmental Management, 188, 9–17. https://doi.org/10.1016/j.jenvman.2016.11.069.

Walker R.T., Solecki W.D., 1999. Managing Land Use and Land-Cover Change: The New Jersey Pinelands Biosphere Reserve. Annals of the Association of American Geographers, 89(2), 220–237. https://doi.org/10.1111/1467-8306.00143.

Xu X., Xie Y., Qi K., Luo Z., Wang X., 2018. Detecting the response of bird communities and biodiversity to habitat loss and fragmentation due to urbanization. Science of the Total Environment, 624, 1561–1576. https://doi.org/10.1016/j.scitotenv.2017.12.143.

Yang D., Song W., 2023. Tracking land use trajectory to map abandoned farmland in mountainous area. Ecological Informatics, 75, 102103. https://doi.org/10.1016/j.ecoinf.2023.102103.

APPENDIX A

Table A.1. Landscape metrics description

Metric	Unit	Value Range	Definition
Area-Edge			
PLAND$^{(C)}$ (Percentage of landscape)	Percentage	0 < PLAND <= 100	PLAND = 0 when the proportional class area is decreasing. PLAND = 100 when only one patch is present.
LPI$^{(C,L)}$ (Largest patch index)	Percentage	0 < LPI <= 100	LPI = 0 when the largest patch is becoming small and LPI = 100 when only one patch is present
ED$^{(C,L)}$ (Edge density)	Meters per hectare	ED >= 0	ED = 0 if only one patch is present and increases, without limit, as the landscapes becomes patchier
Shape			
PARFAC$^{(C,L)}$ (Perimeter-Area Fractal Index)	None	1 <= PAFRAC <= 2	PAFRAC = 1 for patches with simple shapes and approaches PAFRAC = 2 for irregular shapes
SHAPE_MN$^{(C,L)}$ (Mean Shape Index)	None	SHAPE_MN >= 1	SHAPE_MN = 1 if all patches are squares. Increases as the shapes of patches become more complex
FRAC_MN$^{(C,L)}$ (Mean Fractal Dimension Index)	None	FRAC_MN > 0	FRAC_MN = 1 if all patches are squares. It increases as the shapes of patches become more complex
CONTIG_MN$^{(C,L)}$ (Mean Contiguity Index)	None	0 >= CONTIG_MN <= 1	CONTIG_MN assess the spatial connectedness (contiguity) of cells in patches
Aggregation			
NP$^{(C,L)}$ (Number of patches)	None	NP >= 1	NP describes the fragmentation of a class. It equals 1 when only one patch is present and increases as the number of patches increases
PD$^{(C,L)}$ (Patch density)	Number per 100 hectares	0 < PD <= 1e+06	Patch density describes the fragmentation of a class, which increases as the landscape gets patchier
AI$^{(C,L)}$ (Aggregation index)	Percent	0 <= AI <= 100	AI = 0 for maximally disaggregated and 100 for maximally aggregated classes
LSI$^{(C,L)}$ (Landscape shape index)	None	LSI >= 1	LSI = 1 when only one squared patch is present or all patches are maximally aggregated. Increases, without limit, as the length of the actual edges increases, i.e. the patches become less compact
COHESION$^{(C,L)}$ (Patch Cohesion Index)	Percent	0 <= COHESION <= 100	COHESION = 0 if patches of class i become more isolated. It increases if patches of class i become more aggregated
Diversity			
PR$^{(C,L)}$ (Patch richness)	None	PR >= 1	PR = 1 when only one patch is present and increases, without limit, as the number of classes increases
SHDI$^{(L)}$ (Shannon's diversity index)	None	SHDI >= 0	SHDI is equal to zero when there is just one patch present and increases indefinitely when the number of classes increases with proportions being constant
SHEI$^{(L)}$ (Shannons's evenness index)	None	0 <= SHEI < 1	When there is just one patch present, SHEI = 0; when the proportion of classes is distributed equally across all classes, SHEI = 1
(C): Class level metric; (L): Landscape level metric			

Table A2. Accuracy assessment of LULC classification data from 1990 to 2020

Class	1990		2000		2010		2020	
	UA (%)	PA (%)	UA (%)	PA (%)	UA (%)	PA (%)	UA (%)	PA (%)
Aquaculture	86.7	89.7	93.3	93.3	93.3	90.3	93.3	90.3
Bamboo area	95	82.6	95	85.6	95	85.6	94	85.5
Barren land	70	89.7	76	90.5	76	90.5	86	91.5
Evergreen broadleaf forest	84	93.3	84	95.5	84	95.5	84	96.6
Grassland/Herbaceous vegetation	77	91.7	77	90.6	77	90.6	77	90.6
High developed areas	73.3	68.8	73.3	75.9	76.7	76.7	76.7	74.2
Low developed areas	86.7	89.7	90	90	90	87.1	90	87.1
Open water	73.3	88	80	85.7	80	80	80	80
Other croplands	70	65.6	76.7	65.7	83.3	71.4	83.3	73.5
Plantation land	73	67	73	67	77	74	77	74.8
Rice paddies	84	80.8	84	80.8	86	81.1	86	81.1
Scrub/Shrub	94	75.8	94	78.3	94	78.3	94	79.7
Woody crops	76	73.1	76	74.5	76	76	76	77.6
Overall accuracy (%)	**81.07**		**82.4**		**83.47**		**84**	
Kappa coefficient (K)	**0.79**		**0.81**		**0.82**		**0.82**	
Note: UA: User's accuracy; PA: Producer's accuracy								

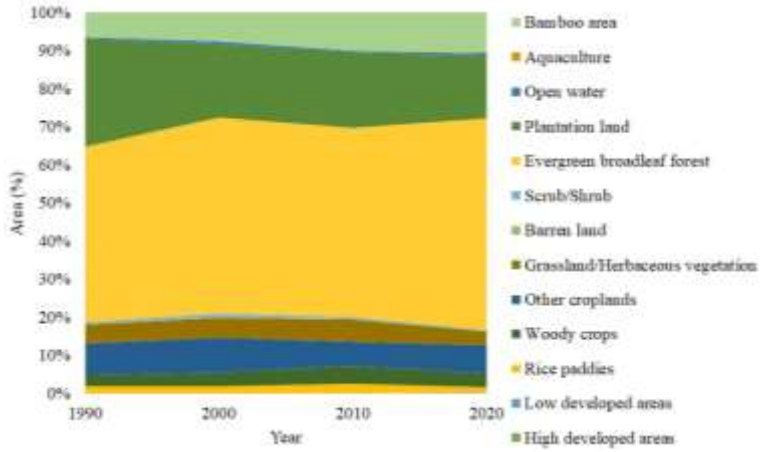

Figure A.1. Distribution of LULC types (in percent) from 1990 to 2020

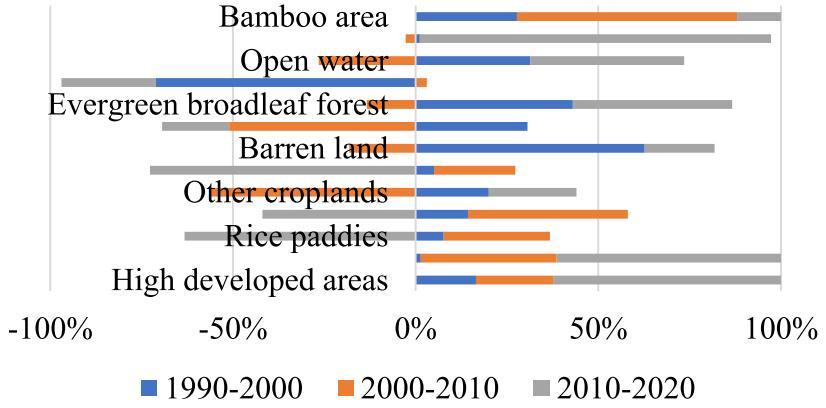

Figure A.2. Change in proportion of LULC categories from 1990 to 2020

Table A.3. Net change (%) of LULC categories from 1990 to 2020

LULC	1990-2000	2000-2010	2010-2020	1990-2020
High developed areas	80.55	11.40	15.71	162.72
Low developed areas	9.43	127.30	15.32	221.75
Rice paddies	0.73	2.58	-4.46	-0.84
Woody crops	1.29	3.50	-2.48	0.49
Other croplands	1.29	-3.20	2.02	-0.26
Grassland/Herbaceous vegetation	0.33	1.39	-4.00	-0.98
Barren land	14.44	-1.71	2.18	4.89
Scrub/Shrub	5.20	-5.70	-4.76	-2.19
Evergreen broadleaf forest	1.23	-0.34	1.15	0.70
Plantation land	-3.18	0.20	-1.67	-1.40
Open water	2.80	-1.85	3.60	1.40
Aquaculture	0.29	-0.66	25.12	7.91
Bamboo area	1.74	3.22	0.48	2.09

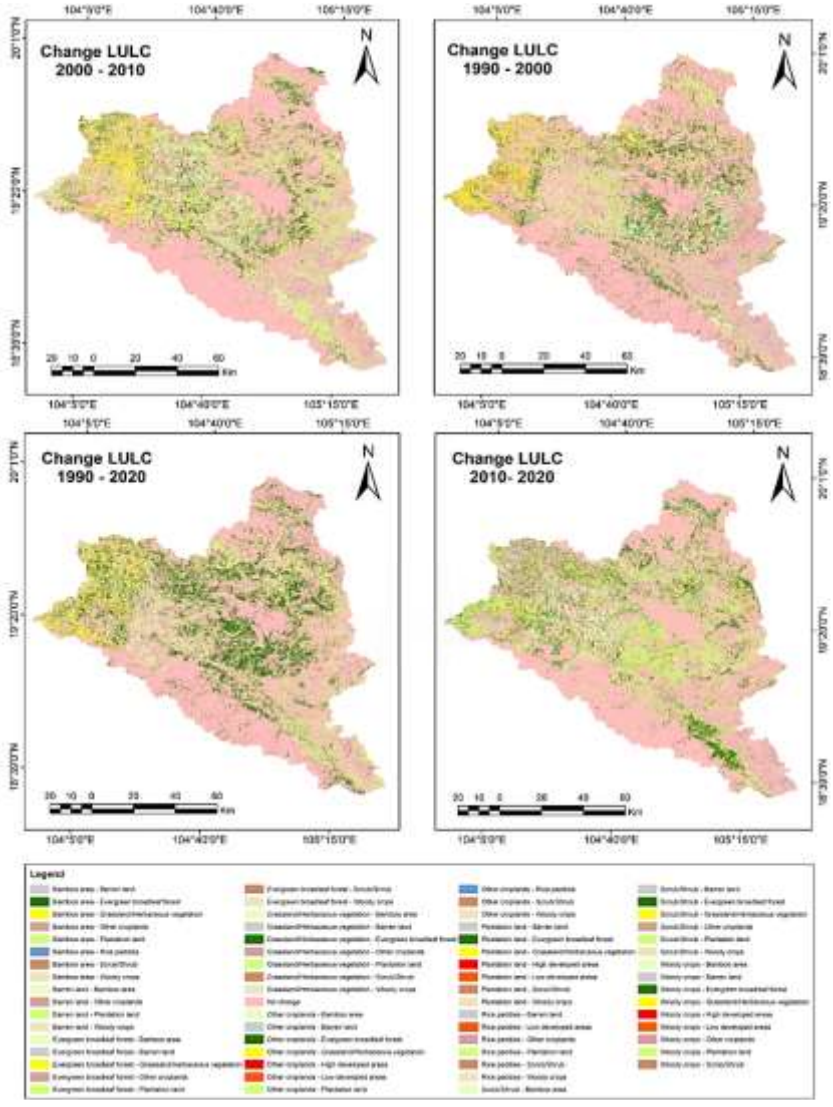

Figure A.3. Land use/land cover change from 1990 to 2020

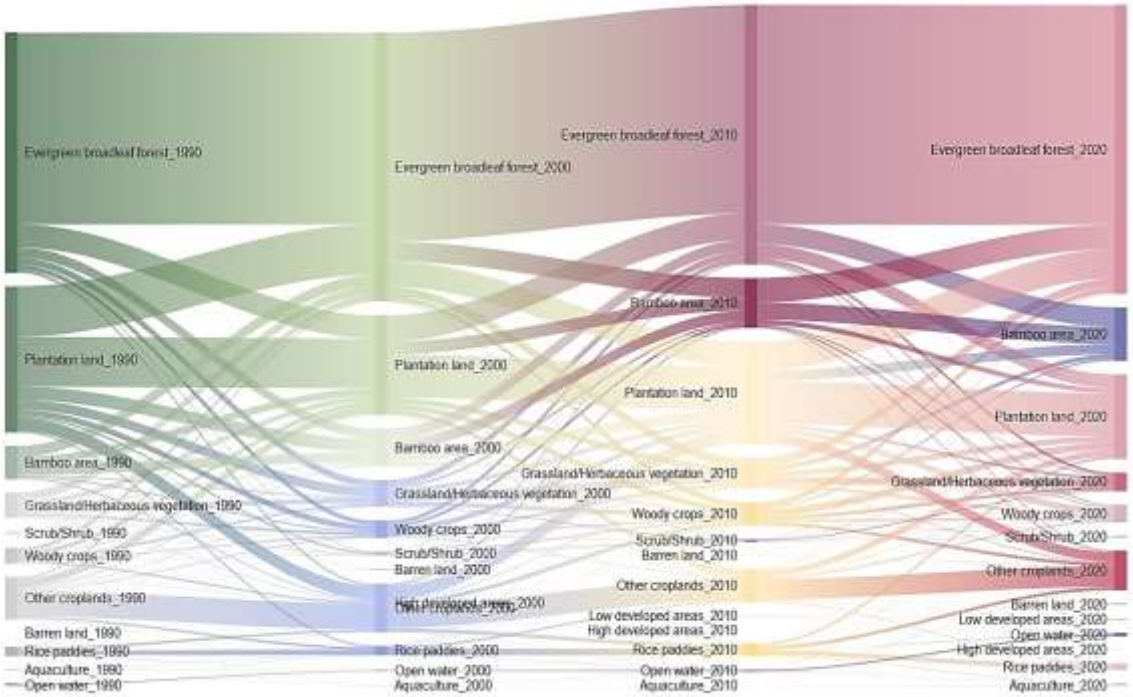

Figure A.4. Temporal gross LULC conversions in WNA. BR. represent transitions among different LULC types from 1990 to 2020

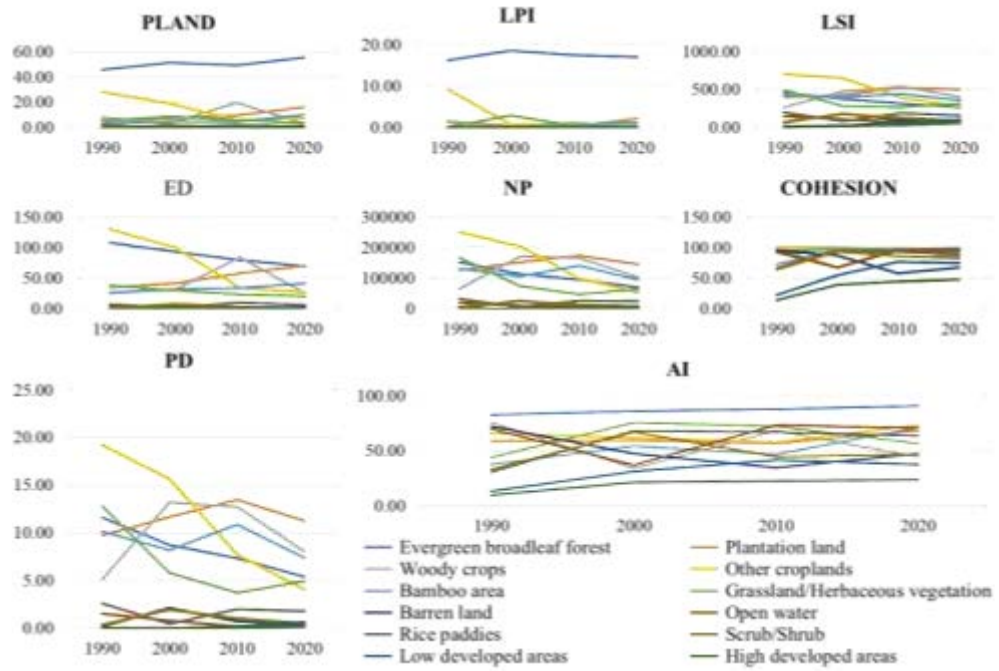

Figure A.5. Change of PLAND, LPI, LSI, ED, NP, COHESION, PD, AI metrics at class level from 1990 to 2020

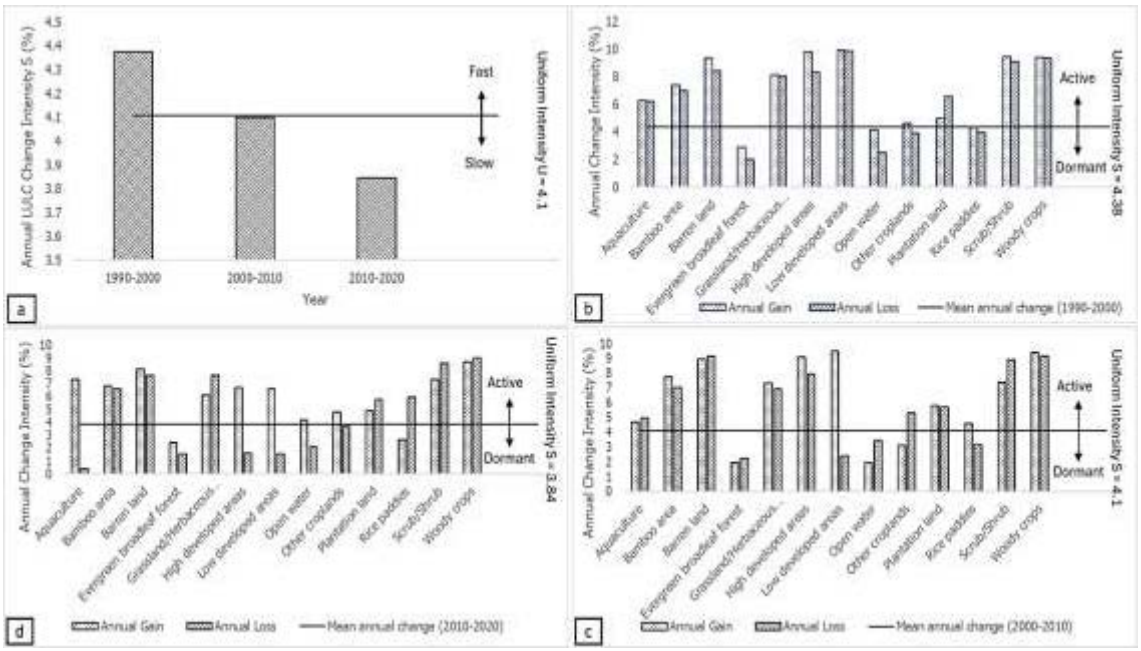

Figure A.6. Land use land cover intensity change of WNABR at the interval time (a) and at category level (b. 1990-2000, c. 2000-2010, and d. 2010-2020)

Table A.4. Calculation results of LULC change intensity and landscape metrics at the landscape level for functional zone from 1990 to 2020

Zone	Year	Area-edge		Shape			Aggregation					Diversity		
		LPI	ED	SHAPE_MN	FRAC_MN	PAFRAC	NP	PD	LSI	COHESION	AI	PR	SHDI	SHEI
TZ	1990	10.45	215.12	1.21	1.04	1.54	372110	81.56	367.11	99.12	68.37	12	1.64	0.66
	2000	5.54	211.31	1.21	1.04	1.53	371609	81.19	361.23	98.85	68.92	12	1.77	0.71
	2010	4.24	199.27	1.22	1.04	1.52	332733	72.7	340.87	98.92	70.68	12	1.8	0.73
	2020	5.11	171.99	1.22	1.04	1.51	268832	58.74	294.74	99.01	74.37	12	1.63	0.66
C1	1990	88.72	81.06	1.17	1.03	1.56	26974	30.24	62.55	99.87	88.09	12	0.40	0.16
	2000	96.22	31.81	1.1	1.02	1.54	15167	16.93	25.82	99.89	95.27	12	0.2	0.08
	2010	95.35	30.38	1.16	1.03	1.52	10658	11.9	24.75	99.88	95.48	11	0.22	0.09
	2020	93.38	30.43	1.23	1.04	1.48	7106	7.93	24.79	99.88	95.47	11	0.26	0.11
C2	1990	87.47	80.68	1.16	1.03	1.55	9765	37.22	34.84	99.67	88.05	10	0.51	0.22
	2000	88.27	53.49	1.18	1.03	1.5	6220	22.83	24.21	99.6	92.05	10	0.5	0.22
	2010	87.99	52.82	1.18	1.04	1.52	6422	23.57	23.94	99.5	92.14	12	0.48	0.19
	2020	90.95	53.3	1.17	1.04	1.51	6729	24.7	24.14	99.67	92.06	12	0.42	0.17
C3	1990	65.71	153.72	1.19	1.04	1.56	23493	59.27	78.47	99.62	77.49	10	0.89	0.39
	2000	85.5	93.97	1.14	1.03	1.54	18114	45.69	48.74	99.73	86.19	10	0.58	0.25
	2010	80.09	88.95	1.22	1.04	1.53	13091	33.02	46.24	99.59	86.93	11	0.66	0.28
	2020	90.09	45.01	1.2	1.04	1.5	6460	16.3	24.37	99.75	93.33	11	0.41	0.17
BZ	1990	12.71	204.98	1.20	1.04	1.55	465316	81.34	391.15	99.41	69.96	12	1.41	0.57
	2000	17.97	188.34	1.2	1.04	1.54	434746	75.83	360.06	99.42	72.38	12	1.39	0.56
	2010	12.46	181.86	1.22	1.04	1.53	383364	66.87	347.8	99.09	73.34	12	1.41	0.57
	2020	9.79	139.17	1.23	1.04	1.52	272024	47.45	266.99	99.26	79.42	12	1.29	0.52

Note: Functional zone of Western Nghe An Biosphere Reserve: TZ: Transitional zone; C1: Core zone 1 - Pu Mat National Park; C2: Core zone 2 - Pu Hoat Nature Reserve; C3: Core zone 3 - Pu Huong Nature Reserve; BZ: Buffer zone